



Contrasting impact of different Mediterranean cyclones on the hydrological cycle and ocean heat content

Yonatan Givon¹, Douglas Keller Jr.², Philippe Drobinski², and Shira Raveh-Rubin¹

¹Department of Earth and Planetary Sciences, Weizmann Institute of Science, Rehovot, Israel

²Laboratoire de Météorologie Dynamique-IPSL, École Polytechnique, Institut Polytechnique de Paris, ENS, PSL Research University, Sorbonne Université, CNRS, Palaiseau, France

Correspondence: Yonatan Givon (yonatan.givon@weizmann.ac.il)

Received: 4 December 2025 – Discussion started: 12 December 2025

Revised: 10 February 2026 – Accepted: 12 March 2026 – Published: 8 April 2026

Abstract. Mediterranean cyclones (MCs) play a crucial role in the Mediterranean hydrological cycle (MHC), driving up to 70% of precipitation and 50% of evaporation totals, and larger fractions of their extremes. Therefore, regional sensitivity to warming is often associated with long-term changes of MCs. These may lead to regional climate feedback through pathways linked directly or indirectly to the MHC: from decreasing cloud cover and precipitation to increased water-vapor uptake. However, the ability of MCs to generate coherent climate feedback is under ongoing debate. Moreover, given the large diversity of processes driving MCs, the role of each in the MHC and their variability remains unexplored. Our recent process-based MC classification allows the breakdown of MC's contribution to the MHC under different dominant cyclogenetic processes. Based on 1-hourly ECMWF ERA5 reanalysis data (1979–2020), 3190 MC tracks are analyzed. We first quantify the total contribution of MCs to the MHC following the cyclone tracks. We analyze the spatial and temporal patterns of the annually accumulated cyclone-induced precipitation (P) and surface evaporation (E). The process-based classification allows the quantification of independent contributions from various cyclone drivers to cyclone-induced P and E and their long-term trends. The results show that the overall annual $P-E$ residual associated with MCs is positive but decreases over time, losing $\sim 0.5 \text{ mm yr}^{-1}$. The classification reveals opposing roles and long-term trends in the annual contributions of each cyclone driver, shifting the balance between cyclone-induced P and E from P -dominated towards E -dominated MCs. These changes are primarily due to reduced precipitation associated with double-jet MCs and daughter

cyclones and increased evaporation associated with thermal lows (-0.2 mm yr^{-1} , each), alternately driven by changes in frequency and/or flux intensities of specific cyclone drivers. Mainly, a sharp rise in frequency affects heat lows, while double-jet cyclones are mostly affected by decreasing precipitation rates. The downward impact of MCs on the Mediterranean Sea heat content also varies sharply between MC types: while MCs generally draw heat from the Mediterranean, certain MC types have the opposing effect, adding further heat. Beyond providing a framework for follow-up analysis of MC impact on the MHC in future climate simulations, the results highlight the independent and opposing contributions of different MC drivers to the Mediterranean heat content, enhancing our understanding of their dynamic response to warming and its impact on society.

1 Introduction

Extratropical cyclones are prominent low pressure weather systems that strongly influence the hydrological cycle, as they drive heavy precipitation (P) and evaporation (E). While the link between cyclones and P is well defined through their forced uplifting, E involves more complex relationships with cyclone-induced perturbations via wind speed, humidity and temperature.

The Mediterranean Sea hosts a unique subset of cyclones in the transition zone between the sub- and extra-tropics. Mediterranean cyclones (MCs) differ from other open-ocean cyclones primarily in their compact spatial structure and the diverse influences of orography, strong land-sea contrast, and

relatively warm sea surface temperatures (Flaounas et al., 2022). As a result, MCs are considered challenging to predict and represent in models on both weather and climate scales (Lionello and Giorgi, 2007; Hatzaki et al., 2023), with their transient manifestation as extra-tropical cyclones, subtropical heat lows, and rare tropical-like cyclones (Flaounas et al., 2015).

Beyond their socio-economic impacts, reviewed recently by Khodayar et al. (2025), MCs have a significant influence on the Mediterranean hydrological cycle (MHC), driving extreme E and P rates and accounting for considerable portions of the overall air-sea exchange of freshwater fluxes (Raveh-Rubin and Wernli, 2015; Lebeaupin Brossier et al., 2015; Flaounas et al., 2016). Due to their dominance on the MHC, long-term variations in features of MCs are often used to explain the regional sensitivity to climate change (Lionello and Giorgi, 2007; Hochman et al., 2020; Reale et al., 2022; Zittis et al., 2022). Specifically, regions prone to moistening are expected to get moister, and vice versa for regions prone to drying. This phenomenon is often referred to as the “wet gets wetter – dry gets drier” mechanism, or the “Mediterranean precipitation paradox”, often explained by a rise in MC-associated P due to increased water-vapor uptake caused by the rise in temperatures under global warming, and a drying effect as MCs become less frequent in the southern and eastern Mediterranean due to the poleward shift of the Atlantic storm track (Chericoni et al., 2025).

However, the direct link to cyclone properties is usually implied rather than shown, and it remains unclear how MCs respond to and affect the regional climate changes through their contribution to P (Zappa et al., 2015; Zittis et al., 2019; Scoccimarro et al., 2025) and E (Flaounas et al., 2019; Reale et al., 2001). While in the tropics enhanced E rates are deemed necessary to sustain cyclones and generate P , in the extra-tropics, extreme evaporation rates may arise preferentially in their cold sector. In the cold sector, under the wake of cyclone and frontal passage, E typically peaks under cold air outbreaks (Papritz et al., 2015; Thurnherr et al., 2021; Aemisegger and Papritz, 2018) and dry intrusions, namely, large-scale descending air streams of extratropical cyclones, that amplify surface evaporation through the penetration of dry air masses with strong wind speeds from upper levels to the surface boundary layer (Raveh-Rubin, 2017; Iltoviz et al., 2021; Rai and Raveh-Rubin, 2023; Klaidier and Raveh-Rubin, 2023; Givon et al., 2024b). While the frequency of MCs is expected to decrease (Nissen et al., 2014), uncertainty exists regarding their projected intensification under global warming, changing their overall contribution to the MHC and being inconsistent among climate models (Gaertner et al., 2007). Lionello et al. (2008) investigated projected changes in cyclone activity over Europe, including the Mediterranean basin, and emphasized the importance of regional characterization of changes in cyclonic activity, due to the large variability among MCs.

Changes in water availability are often measured using the difference between E and P , with recent work (Tootoonchi et al., 2025) indicating MCs (transient eddies) as the major driver of humidity convergence from the ocean sources to adjacent land sinks, pointing out their importance for the atmospheric branch of the MHC. Flaounas et al. (2016) used an intensity-dependent cyclone impact area to analyze the climatological contribution of MCs to the atmospheric MHC in coupled, high-resolution WRF (atmosphere) and NEMO (ocean) simulations. Their results show that up to 90 % of P extremes (95th percentile) and up to 70 % of extreme E rates are associated with MCs. The study further evaluates the annual contribution of MCs to the MHC, suggesting a small residual ($E-P$). They conclude that MCs sustain a balance between their induced E and P on longer time scales, suggesting that changes in their contributions are unlikely to substantially alter the future MHC.

Nevertheless, considering the various manifestations of MCs, it is important to know whether their role in the MHC differs by driving mechanism, as each may pose a different direction of response to climate change. Givon et al. (2024a) revealed the potential of classifying MC tracks by their dominant large-scale driver to enhance the dynamical understanding of MCs and their long-term variability. This classification was adopted by Rousseau-Rizzi et al. (2024), Portal et al. (2024), and Portal et al. (2025) to analyze MC-related compound hazards and extremes (including P) and investigate their convective features. By separating MC tracks into 9 distinct groups indicative of different dominant cyclogenetic processes, the fundamentally different life cycles and weather impacts of each MC driver are revealed, allowing the decomposition of the hydrological contribution of MCs into a spectrum of MC drivers.

Primarily through their intense evaporation rates, MCs (and cyclones in general) are effective at extracting latent and sensible heat from the ocean. While several studies have focused on the cooling effect of regional gap-wind regimes such as the mistral and bora winds (Berthou et al., 2018; Flamant, 2003) on sea surface temperatures, literature focusing on the direct impact of MCs on the ocean heat content (OHC) is scarce. Givon et al. (2024b), for example, systematically analyzed ocean evaporation fluxes associated with the mistral, emphasizing the role of downward advection of upper-level momentum by dry intrusions in the generation of extreme evaporation rates. Keller et al. (2022, 2024) and Keller (2025) further consolidated the importance of the mistral wind to deep water formation in the Gulf of Lion. However, how different MC drivers impact the Mediterranean OHC is not well known. Since OHC is often considered as an energy source for developing MCs (Stathopoulos et al., 2020; Strobach et al., 2024), especially tropical-like ones (“Medicanes”; Cavicchia et al., 2014; Jangir et al., 2024; Miglietta et al., 2025), we aim to evaluate which MC types are the most influential for the OHC in different regions across the Mediterranean basin. Revealing subtle changes in the heat

extraction capacity of MCs is important, as these changes may compromise their climatological role as cooling agents in the oceanic system. Analyzing the impact of the various MC drivers on both the MHC and OHC will allow a better understanding of future changes in the Mediterranean climate. Therefore, our research objectives are threefold:

1. Quantify overall cyclone contribution to the mean annual MHC (P , E and $P-E$), and decompose this to different MC drivers (following Givon et al., 2024a)
2. Reveal historical trends in (1)
3. Evaluate the influence of (1) on the OHC

For this study, we use comprehensive cyclone track data, generated through a composite cyclone detection algorithm (Flaounas et al., 2023) based on ECMWF ERA5 reanalysis (1979–2020) and apply the cyclone-centered potential vorticity (PV) classification presented by Givon et al. (2024a). We define a cyclone impact area to accumulate surface evaporation and precipitation throughout each cyclone track and obtain the cyclone-induced fluxes. We then separate each MC track into the 9 classes and evaluate the long-term trends in the annually accumulated precipitation and evaporation. Finally, we use a NEMO simulation forced by ERA5 to quantify the impact of MCs on the OHC, examining the cyclone-induced heat loss of the Mediterranean.

2 Methods

2.1 Cyclone detection and tracking

MCs are here detected and tracked based on a composite cyclone detection algorithm presented by Flaounas et al. (2023) and used by Givon et al. (2024a) for the dynamic classification of MCs. With this approach, 10 different tracking methods are applied to 1-hourly ERA5 reanalysis of ECMWF (Hersbach et al., 2020). Confidence level 5 is chosen, denoting the agreement of at least 5 detection methods on every MC track. Each composite cyclone track contains the location of its center throughout its lifetime. Sea level pressure at the cyclone center is also reported, and its minimum along the track is used to define MC peak time for classification. Some cyclone tracks that do not cross east of longitude 5° E are removed from the analysis, see more details in Givon et al. (2024a). Overall, 3190 MC tracks are captured throughout the period, with a minimum lifetime of 2 d.

2.2 Process-based classification

Here, we utilize the cluster separation presented in Givon et al. (2024a). Specifically, for each MC at peak intensity, the surrounding upper-level isentropic potential vorticity field (PV, vertically averaged between the 320–340 K isentropic levels) is extracted around the cyclone center. The PV field

is considered within a domain extending 20° east and west of the MC center, 40° to the north and 20° to the south. The PV field is classified using a self-organizing map algorithm (SOM), producing 9 robust clusters with distinct Rossby wave patterns, unique surface impacts, and inherent characteristics. Here, we attribute the cluster number originally determined for the cyclone peak time throughout the cyclone's lifetime.

2.3 MC impact area

We integrate the hourly P and E accumulated along each MC track to derive MC-induced freshwater fluxes. To attribute the fluxes to the MC track and allow an objective comparison of the different MC types we define a constant 10° radius impact area around the cyclone center, within which the fluxes are accumulated in 1-hourly steps along the track. This ensures that no cluster is favored or penalized by impact area differences. While a 10° radius may be considered excessive to associate to MCs (Flaounas et al., 2016), it has been adopted by recent studies on MC impacts (Rousseau-Rizzi et al., 2024; Portal et al., 2024). Results show little sensitivity to the MC impact area in the present framework: with a 5° radius, the spatially accumulated cyclone-induced fluxes naturally decrease, but the fundamental differences among the MC types and their temporal variability are unchanged. Area-weighted averages are calculated across the MC impact area and accumulated annually to quantify total MC-induced fluxes.

To investigate interannual trends in MC-induced evaporation and precipitation, we accumulate freshwater fluxes spatially and temporally across each year, integrating along the MC tracks. We thus obtain a Lagrangian framework used to unveil the cyclone-driven component of the MHC under a process-based prism, resulting in a novel hydrological-budget analysis of differently driven MCs.

2.4 Normalization by MC frequency

As noted by Zappa et al. (2015), changes in MC-induced P are influenced by both changes in MC frequency and intensity. A similar argument can be made for MC-induced E . To address both sources of variance, we complement the accumulated MHC contributions with their normalized ones. To eliminate variations in frequency and obtain the fluxes per cyclone, normalized P and E are evaluated as follows:

$$P_{\text{norm}} = \bar{F}_{\text{MC}} \sum_y \frac{P_y}{F_y} \quad (1)$$

$$E_{\text{norm}} = \bar{F}_{\text{MC}} \sum_y \frac{E_y}{F_y} \quad (2)$$

Where P_y , E_y stands for annual cyclone-induced precipitation and evaporation, respectively, F_y denotes the corresponding annual frequency of MCs, and \bar{F}_{MC} denotes the mean MC frequency across all years. The annual frequency

accounts for the co-occurrence of multiple cyclones in the domain by counting the number of MC centers at every time step. Although this approach leads to large annual frequencies (up to 80 %, as also recognized by Flaounas et al., 2016), it ensures the overall conservation of mass. We similarly normalize the contributions from each cluster to reveal MC types that are more susceptible to these elusive changes in intensity.

2.5 Ocean heat content

Ocean heat content (OHC) in the layer 0–300 m is computed using the Euro-Mediterranean Center on Climate Change (CMCC-Foundation) eddy-permitting global ocean reanalysis, C-GLORS v7. The model data is provided at daily frequency from 1993 up to 2019 and $1/4^\circ$ horizontal resolution with 50 vertical levels. Details on the model and improvements from previous versions are presented by Storto and Masina (2016). While suffering from low temporal resolution and a shorter temporal extent, the model proves valuable for process-based research on heat exchanges, in agreement with comparable independent estimates.

To investigate the impact of the various MC drivers on the OHC, we use a 6 d window centered at the location of each MC at peak intensity times and map the net difference in OHC before and after an MC passage. These differences are accumulated under the impact area at MC peak time on daily resolution and separated by cluster. The OHC is a measure of stored energy. As such, temporal changes in it can be interpreted as energy fluxes and are indeed affected by atmospheric fluxes of both sensible and latent heat. However, the OHC is affected by other processes as well, such as radiative and advective fluxes. Nevertheless, since the presence of MCs potentially influences all of these, and with the presence of cyclones being the only common feature of the observed data, the OHC response is interpreted as MC-driven fluxes for consistency. We thus convert the OHC difference (originally measured in Joules) to units of virtual evaporation rates (E_v , mm yr^{-1}) as follows:

$$E_v = (365 \times \bar{F}_{\text{MC}_d}) \frac{(\text{OHC}_{t_0+3} - \text{OHC}_{t_0-3})}{6[\text{days}] \times L_v} \quad (3)$$

Where \bar{F}_{MC_d} stands for the annual-mean frequency of MCs on daily scale (either as a whole or per cluster) considering only the peak-time (t_0) of each track, and L_v is the latent heat of evaporation. This way, the MC impact on the OHC is comparable to the atmospheric freshwater fluxes.

We note that this analysis does not fully disentangle the impact of the OHC on MCs, that tend to intensify with response to large OHC values. Nevertheless, the temporal evolution of the difference in OHC (not shown) suggests that the OHC response is temporally centered around the passage of MCs and provides a direct measure of the MC-related ocean-heat loss. We interpret the results as the impact of MCs on OHC, while admitting that MC intensity is partially impacted by initially high OHC values. The agreement between

the MC-driven E and OHC response to MC supports this interpretation. In the future, we aim to further address this two-way coupling between MCs and the OHC in a dedicated study.

3 Results

3.1 MCs overall contribution to the MHC

We begin with a climatological overview of the MHC (Fig. 1a and b), followed by the MC contribution to mean annual P and E . Overall, P is shown to mainly affect coastal areas and mountain ridges, reaching values up to 1500 mm yr^{-1} , whereas E dominates over the maritime regions and is minimal over land. In agreement with previous studies (Flaounas et al., 2016; Tootoonchi et al., 2025), the results highlight the prominence of MCs on the MHC, driving up to 70 % of total precipitation and up to 50 % of total surface evaporation in various regions (Fig. 1c and d). While the contribution of MCs to E overlaps well with cyclone density, the peaks of MC contribution to P are shifted eastwards. This is in line with the findings of Saaroni et al. (2010), highlighting the strong dependence of eastern Mediterranean rainfall on MCs. We note that the contribution of MCs to total surface evaporation is about twice their mean frequency, while their contribution to precipitation is about three times higher, indicating that MC-induced freshwater fluxes are strongly concentrated within the MC impact area rather than resulting from random spatial overlaps.

When examining the area-weighted accumulated fluxes in Fig. 2, grid points affected by MCs show higher P and E mean rates compared to the year-round average regardless of MC presence in the domain (compare Fig. 2a and b). While both P and E of MCs (Fig. 2b) are slightly increasing with time, the positive residual ($P-E$) associated with MCs is being gradually eroded. The normalized fluxes (Fig. 2c) reveal a decrease in P and an increase in E per cyclone. Interestingly, the covariance between MC-induced P and E is solely due to their shared MC frequencies, dropping to zero for the normalized E and P (Fig. 2c). This result suggests that instantaneous E and P rates are unconstrained when observed per cyclone, as MCs converge moisture from other sources in addition to their self-induced E to generate heavy P rates. To better understand the sources of these long-term variabilities, we examine the results under the nine dominant MC drivers.

3.2 MC contribution to the MHC by cluster

Under the cyclone-centered PV classification, the complexity and competing effects of the various MC drivers on the MHC is clarified. Figure 3 highlights the variability between the different MC drivers at peak cyclone intensity. Cluster 4, representing fully developed baroclinic MCs, shows the most intense instantaneous E and P fluxes while cluster 6, typically impacting North Africa, is associated with much

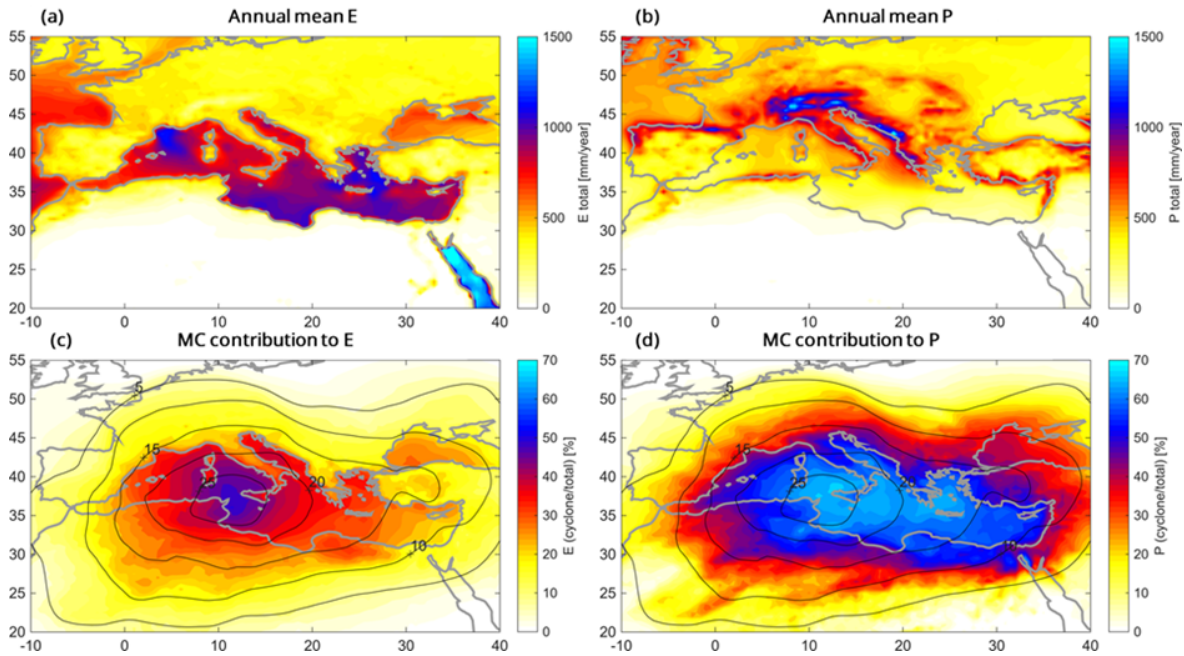


Figure 1. Annual-mean E (a) and P (b), and the relative contribution of MCs to E (c) and P (d) in shading, along with mean cyclone frequency \bar{F}_{MC} (black contours, %).

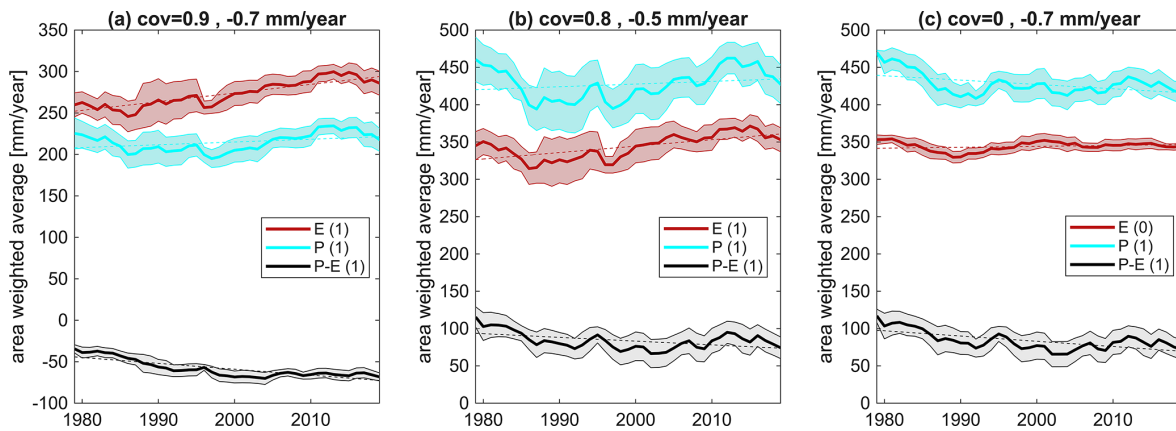


Figure 2. (a) 8-year moving mean (± 1 SD, shading) of total E (red), P (cyan), and $P-E$ (black) within the domain shown in Fig. 1 ($10^\circ E-40^\circ W$, $20-55^\circ N$). Dashed lines denote the corresponding linear best-fit. The result of a 95 % confidence level Mann-Kendall test for each component is shown in the legend (1 for a significant trend). (b) As in panel (a), but for the cyclone-induced E and P , considering only the cyclone impact area. (c) P_{norm} , E_{norm} , i.e., as in panel (b) but normalized by annual cyclone frequency (hourly, including double counts), representing flux intensities. Titles denote the covariance factor between P and E followed by the slope of the linear best-fit (mm yr^{-1}) for the $P-E$ trends.

weaker freshwater exchanges. However, sharp differences are also evident between clusters that share similar seasonal and geographical amplitudes, such as clusters 1, 2, and 4, and clusters 3, 5, and 7. Cluster 8, associated with narrow, cyclonically curving PV streamers, and recently found to be the most favorable for deep convection (Portal et al., 2025), notably exhibits the most intense fluxes among the off-winter clusters.

We note that the impact area well captures the E and P features associated with MCs. The relatively strong evaporation observed about 15° to the west of the MC centers of clusters 3, 5, and 7 (i.e., outside of the impact area) mostly occurs over the Atlantic Ocean, given their preferred locations (black contours in Figs. 4 and 5 and Fig. 7 in Givon et al., 2024a in more detail). With this MC-centered view it appears that a first-order correlation exists between instantaneous MC induced E and P . However, since some of the

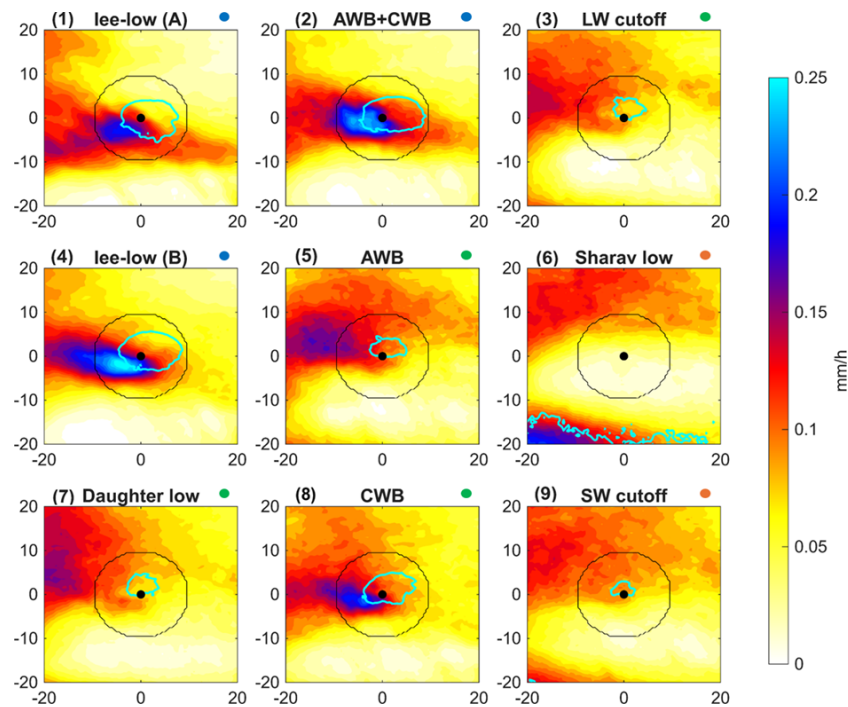


Figure 3. Cyclone-centered cluster composites of E (shading) and P (cyan contours, 0.25 mm h^{-1}) at classification time (minimum SLP time of each MC track). The black circles denote the 10° radius impact area considered for cyclone-induced fluxes. Colored circles indicate the dominant season for each cluster: blue for winter, red for summer, and green for spring/autumn.

clusters appear more frequently on land, we next evaluate the accumulated fluxes throughout the MC duration and consider their geographical areas of influence.

The independent contributions of each MC type to the overall annual E are shown in Fig. 4. Cluster 4 stands out as a major contributor, accounting for up to 24 % of the MC-induced E despite forming 20 % of the total MC frequency (see Fig. 4 titles). The ratio between the MC contribution and local frequency surpasses 3 in the eastern Mediterranean and along the north African coast, suggesting high conditional probability. Cluster 1, representing cold cyclones anchored to topography, shows significant E contributions especially in the Ligurian and Adriatic seas, as may be expected from the strong gap-winds regimes triggered at the early stages of Alpine lee-cyclogenesis and their link to evaporation (Buzzi et al., 2020; Givon et al., 2021, 2024b). On the other hand, the contributions of summer clusters 6 and 9 are weaker than their mean frequency, which is often over land, possibly due to already high evaporation rates throughout the season (Ruiz et al., 2008). Nevertheless, Sharav lows (North-African heat lows captured by cluster 6) are associated with strong evaporation hot-spots in north-western Africa, possibly affecting the great lakes and land-moisture in the region (Rieder et al., 2025). Cluster 2 MCs are denoted by a unique combination of anticyclonic and cyclonic Rossby wave breaking simultaneously deforming the same PV streamer, that extends from the anti-cyclonic shear zone of the sub-polar jet to the north

to the cyclonic shear zone of the sub-tropical jet to the south (Fig. A1). The double-jet configuration denoted by cluster 2 notably contributes 15 % to total MC-induced evaporation despite its 12 % relative frequency, suggesting strong – yet apparently more local – evaporative capabilities, appearing as relatively sporadic evaporation hotspots.

The cluster-separation of contributions to P is even more pronounced (Fig. 5). Cluster 4 dominates in the central and eastern Mediterranean, overall contributing 28 % of total MC induced P , and cluster 1 in the western coasts of Italy, Greece and Turkey, and along the Adriatic, providing 22 % of total MC induced P . The precipitation induced by cluster 2 again exhibits more localized hot spots, while the contributions of the other clusters are significantly weaker. Intriguingly, precipitation along the Egyptian coast shows a tight link to cyclonic wave breaking (CWB) MCs captured in cluster 8, with ~ 20 % of annual precipitation delivered in a mere 1 % regional cluster frequency. Moreover, this region is hardly responsive to other MC clusters. The tight connection between RWB patterns and extreme precipitation were recently highlighted by de Vries (2021), especially for semi-arid areas such as the eastern-Mediterranean.

These results illustrate well the robustness of the PV clustering even beyond the classification time, with profound implications on geographical, seasonal, and dynamical variability. Each MC driver thus plays a fundamentally different role in shaping the MHC.

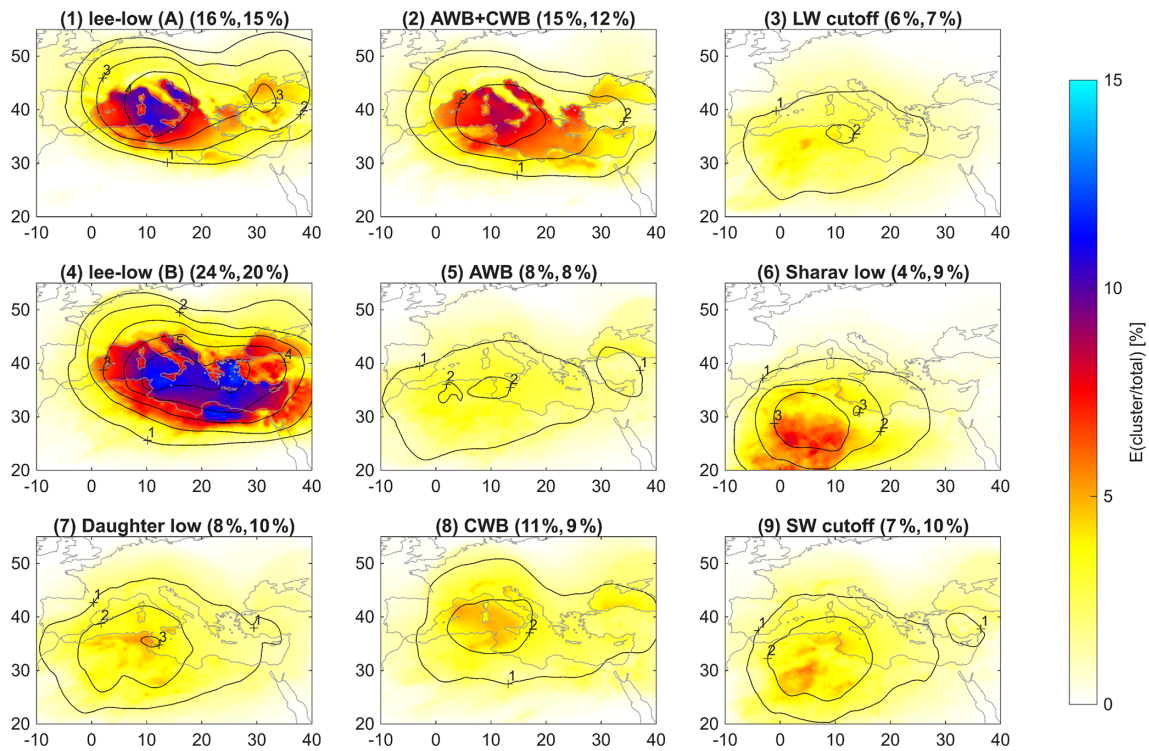


Figure 4. Relative contribution of each cluster to total E (shading, %) and cluster mask frequency (black contours, %, in 1% intervals). Titles denote cluster numbers and the dominant driving mechanism as reported in Givon et al. (2024a). Numbers in brackets indicate the mean contribution of each cluster to total MC-induced surface evaporation (left) and the mean cluster frequency out of all MCs (right).

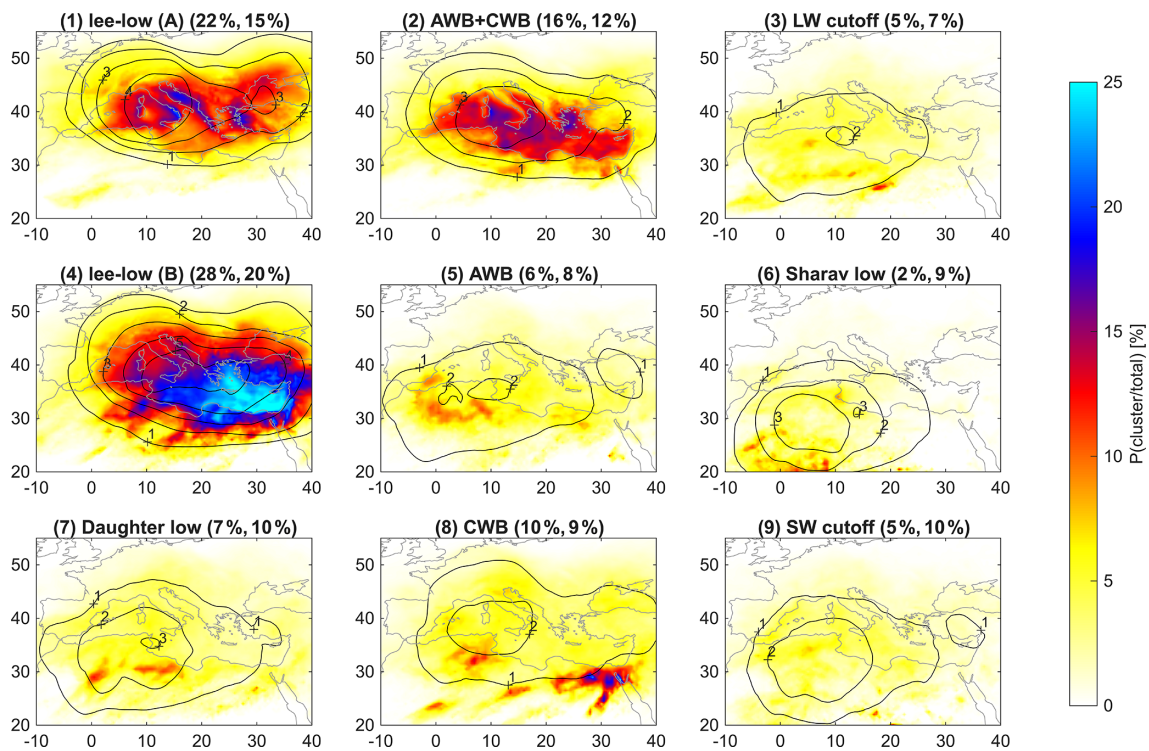


Figure 5. As Fig. 4 but for P .

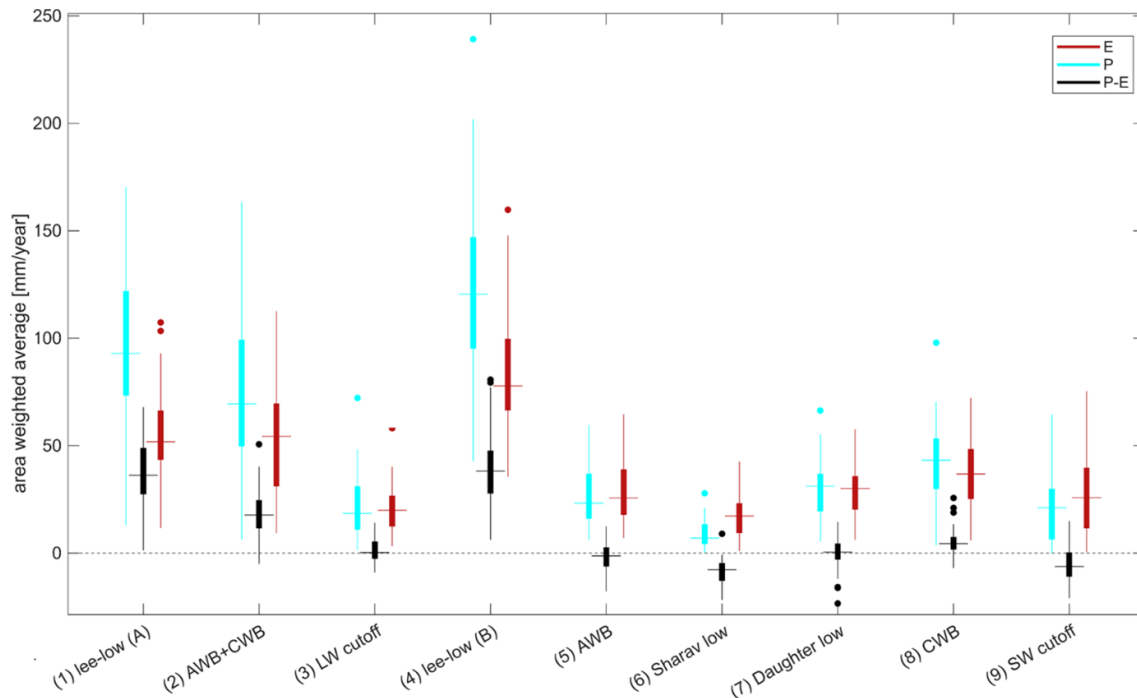


Figure 6. Distributions of area weighted annual mean MC-induced E , P , and $P-E$, separated by cluster. The medians of each distribution are denoted by the horizontal lines, the boxes mark the 25 to 75 percentiles of the distribution, and whiskers mark the 2.5 and 97.5 percentiles, setting the threshold for outliers, marked by the colored dots.

To evaluate the total contribution of MCs and their drivers to the MHC, we accumulate the fluxes spatially and temporally across the years, analyzing both annual P and E distributions as well as their difference, $P-E$, per cluster. Figure 6 shows that the overall slightly positive $P-E$ contribution of MCs is the result of a delicate balance between inherently imbalanced MC contributions: while winter clusters 1, 2, and 4 act as moisture sources, each adding about 30 mm yr^{-1} per grid-point within a 10° radius impact area, these inputs are partly offset by a consistent drying effect imposed by the summer-prone clusters 5, 6, and 9. Seeing as the relative frequencies of each cluster are changing in recent decades (Givon et al., 2024a), we further analyze the long-term variability of each cluster, accounting for both variations in frequency and intensity.

3.3 Long-term variability by cluster

Long term variability of MC occurrence and interaction with the MHC strongly depends also on MC cluster type. The relative importance of each MC cluster is shifting over recent decades, as shown in Fig. 7. While some clusters are well balanced and hardly contribute to the MC-induced $P-E$ (e.g., clusters 5 and 9), $P-E$ is growing larger for some (clusters 1, 3, and 8) and smaller for others (clusters 2, 4, 6, and 7). The strongest change is captured for the double-jet cluster 2, losing 0.2 mm yr^{-1} which corresponds to $\sim 1\%$ erosion of its annual precipitation surplus per year, with similar trend

magnitudes reported for clusters 6 and 7. The net negative contributions from clusters 2, 4, 6, and 7 differentially stem from either a reduction in precipitation (clusters 4 and 7), an increase in evaporation (6), or both (cluster 2). By contrast, cluster 8 contribution is positive and slightly increasing with time, due to enhanced P and near-constant E . As these changes can arise from either changes in frequency or intensity, we next examine the normalized fluxes and their trends, effectively eliminating frequency changes and highlighting changes in E and P intensities.

Indeed, the net contributions ($P-E$) of each cluster vary differently when only changes of flux intensity are considered (Fig. 8). The intensity-only loss from cluster 2 is enhanced to -0.5 mm yr^{-1} , indicating that its increasing frequency masks a drop in intensity. Interestingly, the E_{norm} and P_{norm} associated with cluster 2 evolve in opposite directions, with decreasing P_{norm} (and increasing E_{norm}). As suggested by previous studies, the overall drop in precipitation for cluster 4 is indeed driven solely by a reduction in frequency, while the intensity of both E_{norm} and P_{norm} steadily increase. For cluster 6, changes in intensity exist but are well balanced, suggesting changes in frequency are dominant in determining $P-E$ for these Saharan heat lows.

When separated by cluster, the $P-E$ residual shows distinct long-term trends that are affected by variations in both frequency and intensity. In agreement with previous studies, winter MCs grow in intensity and decrease in frequency, with

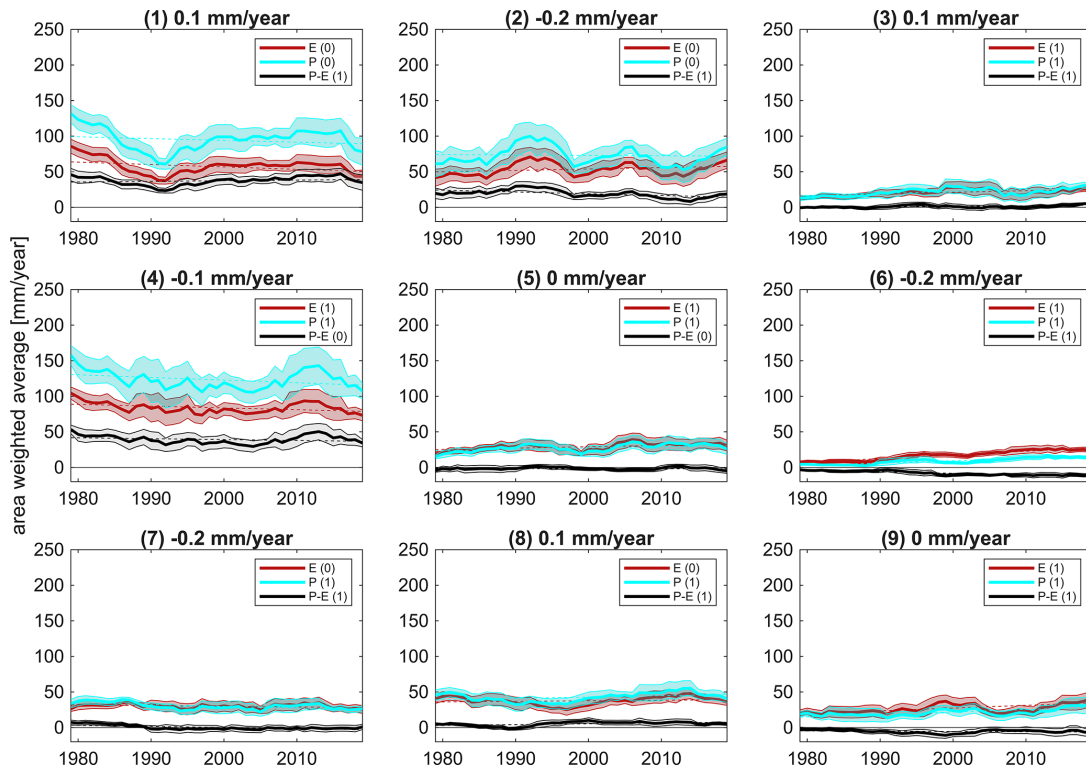


Figure 7. As Fig. 2b but separated by cluster. Titles denote the cluster number followed by the slope of the linear best-fit (mm yr^{-1}) for the $P-E$ trend. The result of a 95 % confidence level Mann-Kendall test for each component is shown in the legend (1 for a significant trend).

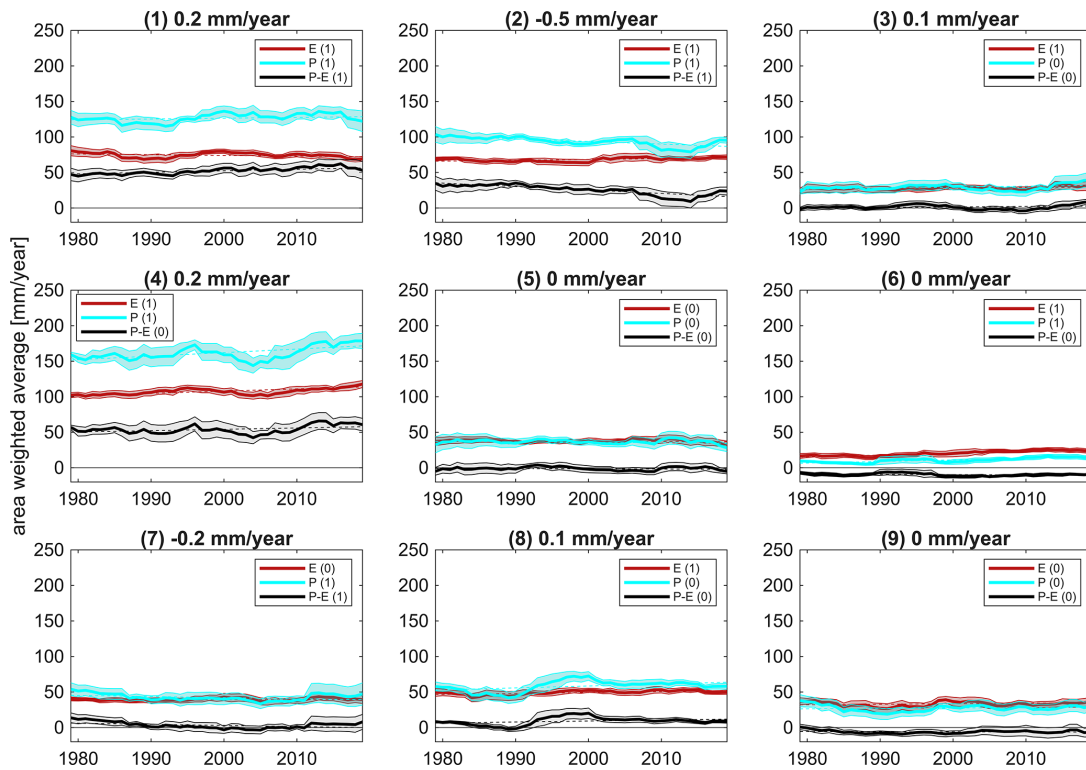


Figure 8. As Fig. 7 but normalized by cluster frequencies, highlighting flux-intensity variations.

Table 1. Total cluster spatio-temporal frequencies and corresponding MHC contributions relative to the total accumulation of the climatological values across the domain. Note that the spatio-temporal frequencies include the fraction of MC-affected grid-points to all grid-points in the domain, as well as their mean temporal frequencies. “All” stands for all MC clusters combined.

Cluster	Net Freq. (%)	<i>E</i> (%)	<i>P</i> (%)	<i>P</i> – <i>E</i> (%)
1	2.0	2.6	5.1	10.7
2	1.6	2.5	4.0	5.5
3	0.9	0.9	1.2	0.6
4	2.6	3.9	6.6	10.4
5	1.1	1.2	1.4	–0.2
6	1.2	0.7	0.5	–2.2
7	1.3	1.3	1.6	0.3
8	1.3	1.7	2.2	1.4
9	1.3	1.2	1.1	–1.4
All	13.4	15.5	22.9	24.1

the latter being more dominant, resulting in a long-term reduction in *P*–*E*. Summer MCs, on the other hand, are primarily affected by a rise in frequency, leading to further drying.

To derive the overall impact of MCs on the MHC, net cluster frequencies and their area weighted contributions to the MHC relative to accumulated climatological values across space and time are shown in Table 1. The net frequencies consider the temporal occurrence of each MC cluster and the ratio between the number of grid-points within the MC masks to the total number of grid points in the domain. These frequencies hence describe the fraction of MC affected areas throughout the entire analysis period and across the whole domain. The overall net climatological *P*–*E* in the Mediterranean is -52 mm yr^{-1} (Fig. 2a). The overall MC-induced *P*–*E* is, however, positive, counter balancing 24 % of the climatological negative *P*–*E*. The MC contribution is primarily driven by lee-cyclones (clusters 1 and 4), while specific MC drivers (clusters 5, 6 and 9) act to enhance the overall excess *E* in the Mediterranean.

3.4 MC-induced OHC perturbations

The overall impact of MCs on the OHC (Fig. 9) shows that on average, MCs extract heat from the Mediterranean at a mean rate equivalent to 645 mm yr^{-1} of *E*. Although other processes affect the OHC, including lateral advection and radiative effects, the contribution of MC induced *E* alone accounts for up to $\sim 350 \text{ mm yr}^{-1}$ (Fig. 2), more than 50 % of the net OHC difference with response to the passage of MCs. Notably, the OHC response to MCs is positive along the North-African and eastern Mediterranean coasts, suggesting MCs tend to add heat to these areas. While this local reversal could be the result of sensible heat fluxes triggered by

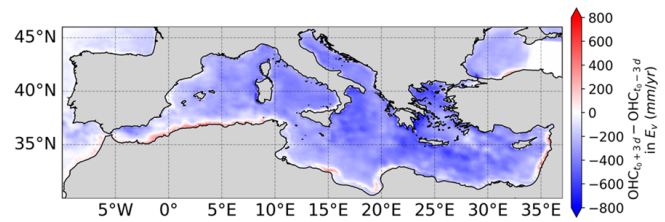


Figure 9. Composites of the difference in ocean heat content ± 3 d before and after the influence of a MC, normalized by annual MC frequencies. Negative values indicate net heat extracted from the ocean towards the atmosphere.

heat lows that often affect these areas, further research into oceanic flows is required to definitively explain these signals.

Once more, the cluster breakdown provides a more detailed picture of the independent role of MC types (Fig. 10): MC drivers that provide excess *P* also appear to drain heat from the ocean (clusters 1, 2, 4, and 8), as their *E* is still higher than that of *E*-dominated MCs. The *E*-dominated MCs (clusters 6, 7, and 9) act as heat sources, enhancing the OHC as they evolve rather than lowering it. This may be the result of their dry formation environments, prohibiting precipitation and leading to convergence of dry, warm air towards the MC center, generating enhanced downward sensible and possibly radiative (i.e., reduced cloud cover) fluxes. Spatial variability is evident for some of the clusters, suggesting certain drivers, e.g. clusters 3 and 5, act differently in different regions. Specifically, these MCs act as heat extractors when impacting the eastern Mediterranean, and heat suppliers when impacting the western parts. The OHC response to the various MC drivers is in-line with the atmospheric perspective, suggesting that opposing contributions of MCs to the MHC also bear the opposite impact on the OHC. This highlights the importance of considering the internal variability of MCs when assessing their role in future climate.

4 Discussion

This work investigates the impact of MCs on precipitation (*P*), evaporation (*E*), and the *P*–*E* residual as well as Mediterranean ocean heat content (OHC), separating between the independent contributions of 9 dominant MC “types”. MCs account for up to 70 % of annual *P* and 50 % of annual *E* (locally, see Fig. 2), but the contribution to each component is highly asymmetric when separated by MC type, as captured by the cyclone-centered PV-based clusters (Givon et al., 2024a). Cluster-dependent trends in cyclone-induced *P*, *E*, and *P*–*E* are revealed, controlled both by changes in MC cluster frequencies and in instantaneous flux intensities. The net annual *P*–*E* of MCs is positive and slightly decreasing due to a decrease (increase) in frequency of winter (summer) MCs. This trend is corroborated

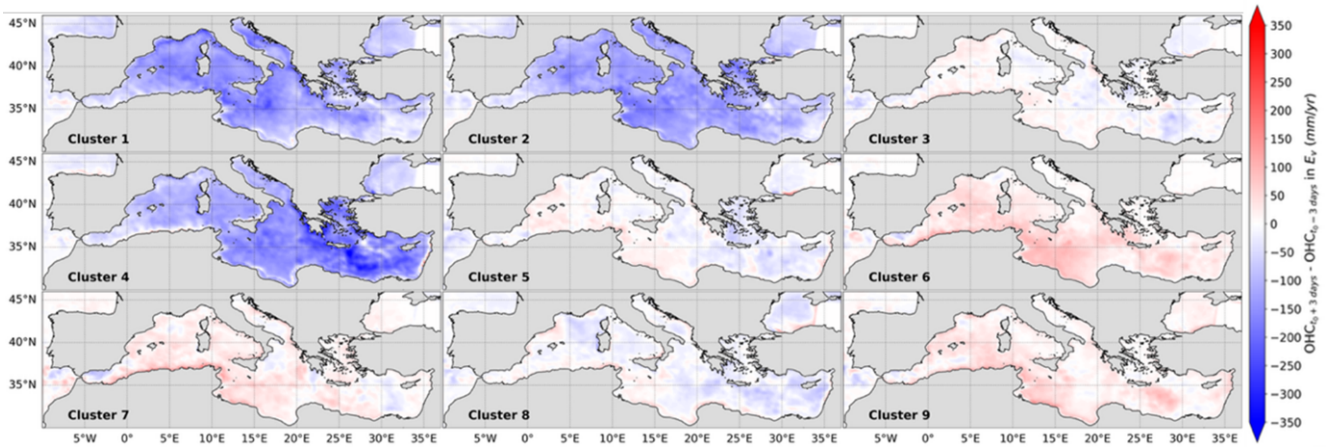


Figure 10. As Fig. 9 but separated into clusters. Note that the values are normalized by annual MC cluster frequencies, thus representing the net heat taken from (negative values) and added to (positive values) the Mediterranean per cluster, per year.

rated by an unbalanced reduction in precipitation intensity associated with intense and compact MCs that evolve under a double-jet configuration (Fig. A1). The results highlight the individual role and potential response of each MC type in the MHC in recent decades, and underline multiple dynamic relationships.

The growing negative contribution of summer MCs to $P-E$ (clusters 6 and 9) reflects both their higher frequency and the rise in sea surface temperature, which enhances E over longer timescales by amplifying air-sea temperature gradients (Yu, 2007). The major winter clusters 1 and 4 play different roles in the MHC despite their apparent similarity. Cluster 1 consistently provides excess P and is mostly restricted to topography, exhibiting no long-term trend in intensity or annual $P-E$ contributions. Cluster 4, on the other hand, travels farther from its genesis region (mostly the lee of the Alps) and delivers excess P to the central and eastern Mediterranean, at a gradually decreasing rate. Cluster 8, although rare, contributes substantially to $P-E$ and shows a distinct increase in P intensity, likely reflecting enhanced convective activity in response to rising surface temperatures – consistent with its high convective potential (Portal et al., 2024). Finally, cluster 2 shows the steepest trend in $P-E$, losing $\sim 0.2 \text{ mm yr}^{-1}$ per affected grid-point, due to changes in mean intensity, despite a subtle rise in frequency.

The seasonal cycle is embedded in the cluster separation. To isolate the role of seasonality, the results were further separated into winter and summer subgroups, specifically November through March and May through September (not shown). While summer E is weaker across all clusters, the relative impact of each cluster as well as the spatial patterns remain surprisingly similar in both sub-groups. Specifically, cluster 4 still shows the largest instantaneous fluxes, followed by clusters 2 and 1. Winter cluster 6 cyclones are especially rare, while cluster 8 is more evenly distributed between the seasons and shows similar E and P patterns (not shown).

We conclude that a further seasonal breakdown does affect the results quantitatively, but not qualitatively with respect to the relative importance of each MC type. This shows that MC types exhibit consistent features across seasons.

The OHC analysis further emphasizes the independent role of each MC driver, with opposing impacts of different MC drivers across the basin. The overall OHC loss is proportional to MC-induced E , but is generally higher due to added sensible, radiative and advective fluxes, all of which are potentially affected by the presence of MCs. We show that certain MCs, primarily RWB patterns and cut-off lows, may even add heat to the Mediterranean instead of extracting it, stressing the importance of non-linear PV dynamics to the OHC.

Overall, the study reveals that each MC driver contributes differently to the MHC and OHC, with some drivers showing opposing long-term trends. These trends are in-line with the Mediterranean precipitation paradox, demonstrating the different dynamical responses generating it: North-Mediterranean winter MCs are indeed showing increased precipitation rates despite their drop in frequency, while off-winter MCs frequently impacting the southern and eastern Mediterranean are increasing in frequency and evaporation rates at the expense of precipitation intensities, contributing to the drying of these regions.

The impact of MCs on the MHC agrees with the trends of total regional P derived by André et al. (2024). The “all quartiles increase” pattern, describing an increase in all precipitation quartiles (i.e., extreme and moderate values alike, not restricted to the occurrence of MCs) suggested for the European continent can be related to the increased P of clusters 1 and 4 often affecting the area. However, the decrease in clusters 2, 6, and 9 partially explain the reduction in P intensity across the central, eastern, and southern parts of the domain.

Taken together, the results show that quantifying the climate impact of MCs requires a process-based approach that resolves their internal diversity. Each cyclogenetic process responds differently to warming, leading to opposing influences on both the MHC and OHC. Long-term trends imply that the warming buffer provided by MCs is being eroded, with severe implications for the regional hydrological budget and heat balance. Moreover, changes in MCs impact on the MHC could develop nonlinearly in the future, as shifts in both frequency and intensity align with ongoing warming for several MC drivers. *E.g.*, winter cyclones do not only drop in frequency or intensity – they are being replaced by MCs with an opposing sign of MHC impact.

The presented framework for the process-based classification and impact attribution presented here is not only relevant for the Mediterranean but also transferable to other regions where cyclones play a critical role in regulating hydroclimate and air-sea exchanges. Applying this methodology more broadly represents a promising avenue for future research.

Appendix A: PV-based clusters of MCs

To provide context for the MHC results by MC cluster, we summarize the PV-based MC cluster characteristics in Givon et al (2024a). The classified PV patterns are shown in Fig. A1 as cyclone centered composite means, depicting the different large-scale settings associated with peak time of each MC track. These include long and short-wave cut-off structures observed for clusters 3 and 9, the anticyclonic and cyclonic Rossby wave breaking patterns for cluster 5 and 8, respectively, and the daughter-cyclone highlighted by cluster 7. Intriguingly, from the cyclone-centered, upper-level PV perspective, clusters 1 and 4 differ only slightly. However, this seemingly subtle difference effectively distinguishes between two stages of lee cyclogenesis (Givon et al., 2024a). The cyclone-centered composite of 300 hPa winds (Fig. A1) visualizes the double-jet pattern associated with cluster 2 MCs, supporting anticyclonic and cyclonic Rossby wave breaking on the poleward and equatorward flanks of the PV streamer, respectively. This unique set-up leads to the extension of the PV streamer furthest equatorward with respect to the sub-polar jet hence generating maximum PV anomalies and surface winds compared to the other clusters. Based on these and other observed features explored in Givon et al (2024a), each cluster is named after its dominant cyclogenetic process. These processes are not limited to specific non-linear RWB life cycles (see panel titles) but also include thermal (Sharav) lows with weak upper-level forcing forming in a ridged environment (cluster 6) and secondary cyclones forming along the fronts of synoptic-scale cyclones (cluster 7).

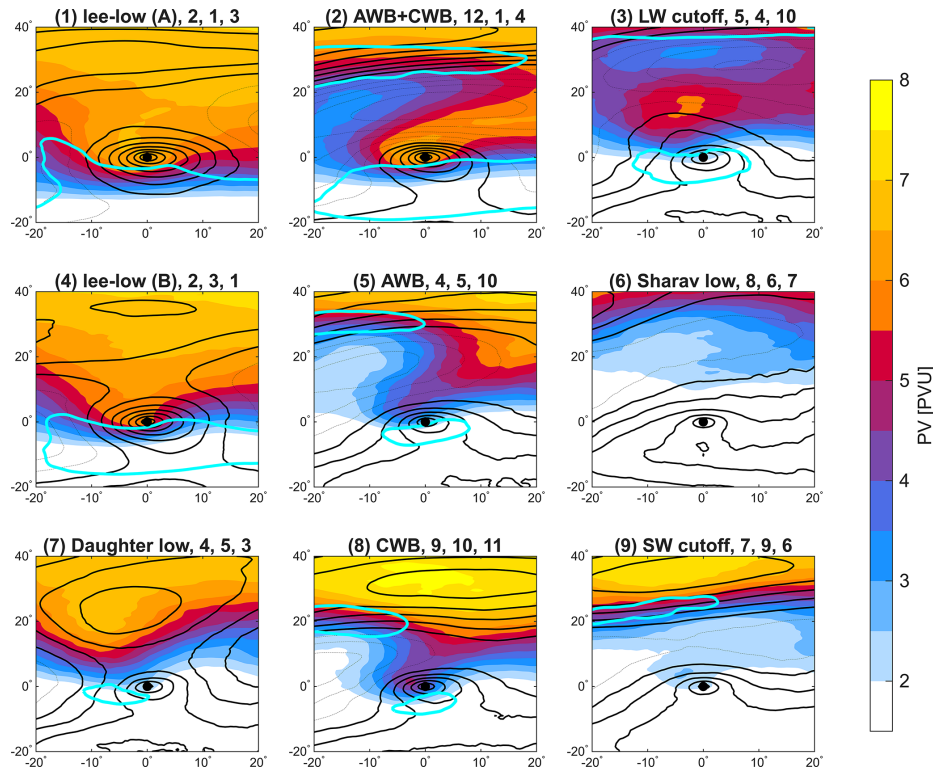


Figure A1. Cyclone-centered cluster composites of upper-level (320–340 K averaged) PV (PVU, shading) and SLP (black contours at 2 hPa intervals, dashed above 1015 hPa) at minimum SLP time. Overlaid is the corresponding composite of the 30 m s^{-1} isotach on the 300 hPa geopotential surface (cyan contour, roughly denoting the subpolar and/or subtropical jets). Titles denote cluster number, name, and the leading cluster months in a descending order.

Data availability. The composite cyclone tracks with the resulting cluster attribution are available in the supplementary assets of Givon et al. (2024a). The track labels correspond to the composite cyclone track dataset at confidence level 5, made available as a Supplement by Flaounas et al. (2023, “TRACKS_CL5.dat”). ERA5 data are available at: <https://doi.org/10.24381/cds.adbb2d47> (Hersbach et al., 2023), and details on C-GLORS v7 data availability can be found at <http://c-glors.cmcc.it/index/index-7.html?sec=7> (last access: 29 March 2026).

Video supplement. An illustrative animation of MC-induced evaporation fluxes throughout the year 2019 is provided (<https://doi.org/10.5446/72785>, Givon, 2026). The evaporation field is cropped within a 10° radius circle surrounding the cyclone centers, in hourly intervals, throughout each cyclone track. The fluxes are accumulated throughout the analysis period and reported as MC-induced E . The equivalent accumulated precipitation is used to define MC-induced P .

Author contributions. YG and SRR conceptualized the research. YG conducted the research, performed the analysis of the atmospheric data, and wrote the underlying codes and the manuscript. DKJ performed the OHC analysis and produced the corresponding figures. All coauthors took active part in reviewing and editing the final draft.

Competing interests. At least one of the (co-)authors is a member of the editorial board of *Weather and Climate Dynamics*. The peer-review process was guided by an independent editor, and the authors also have no other competing interests to declare.

Disclaimer. Publisher’s note: Copernicus Publications remains neutral with regard to jurisdictional claims made in the text, published maps, institutional affiliations, or any other geographical representation in this paper. The authors bear the ultimate responsibility for providing appropriate place names. Views expressed in the text are those of the authors and do not necessarily reflect the views of the publisher.

Acknowledgements. This work stems from the COST Action CA19109 European network for Mediterranean cyclones in weather and climate (Hatzaki et al., 2023), supported by the European Cooperation in Science and Technology (COST; <https://www.cost.eu>, last access: 4 November 2025). We acknowledge the Israel Meteorological Service for granting access to ECMWF. The authors wish to acknowledge Enrico Scoccimaro and Dorotea Ciro Iovino of the Euro-Mediterranean Center on Climate Change (CMCC) for providing the OHC data of C-GLORIS V7, and thank them for their insightful input on an earlier version of the manuscript. The authors wish to thank the two anonymous reviewers for their constructive comments that improved the clarity of the manuscript.

This work was funded by the Israel Science Foundation (grant no. 1242/23) and the De Botton Center for Marine Science at the Weizmann Institute of Science. This work contributes to the Med-World and Tuning for Deserts Consortia, funded by the Council for Higher Education in Israel.

Financial support. This research has been supported by the Israel Science Foundation (grant no. 1242/23) and the Council for Higher Education, Israeli Centers for Research Excellence (grant no. Med-World and Tuning for Deserts Consortia).

Review statement. This paper was edited by Silvio Davolio and reviewed by two anonymous referees.

References

- Aemisegger, F. and Papritz, L.: A Climatology of Strong Large-Scale Ocean Evaporation Events. Part I: Identification, Global Distribution, and Associated Climate Conditions, *J. Climate*, 31, 7287–7312, <https://doi.org/10.1175/JCLI-D-17-0591.1>, 2018.
- André, J., D'Andrea, F., Drobinski, P., and Muller, C.: Regimes of precipitation change over Europe and the Mediterranean, *J. Geophys. Res.-Atmos.*, 129, e2023JD040413, <https://doi.org/10.1029/2023JD040413>, 2024.
- Berthou, S., Mailler, S., Drobinski, P., Arsouze, T., Bastin, S., Beranger, K., and Lebeauin Brossier, C.: Lagged effects of the Mistral wind on heavy precipitation through ocean-atmosphere coupling in the region of Valencia (Spain), *Clim. Dyn.*, 51, 969–983, <https://doi.org/10.1007/s00382-016-3153-0>, 2018.
- Buzzi, A., Davolio, S., and Fantini, M.: Cyclogenesis in the lee of the Alps: a review of theories, *B. Atmos. Sci. Technol.*, 1, 433–457, <https://doi.org/10.1007/s42865-020-00021-6>, 2020.
- Cavicchia, L., von Storch, H., and Gualdi, S.: Mediterranean Tropical-Like Cyclones in Present and Future Climate, *J. Climate*, 27, 7493–7501, <https://doi.org/10.1175/JCLI-D-14-00339.1>, 2014.
- Chericoni, M., Fosser, G., Flaouanas, E., Gaetani, M., and Anav, A.: Unravelling drivers of the future Mediterranean precipitation paradox during cyclones, *npj Clim. Atmos. Sci.*, 8, 260, <https://doi.org/10.1038/s41612-025-01121-w>, 2025.
- de Vries, A. J.: A global climatological perspective on the importance of Rossby wave breaking and intense moisture transport for extreme precipitation events, *Weather Clim. Dynam.*, 2, 129–161, <https://doi.org/10.5194/wcd-2-129-2021>, 2021.
- Flamant, C.: Alpine lee cyclogenesis influence on air-sea heat exchanges and marine atmospheric boundary layer thermodynamics over the western Mediterranean during a Tramontane/Mistral event, *J. Geophys. Res.*, 108, 8057, [10.1029/2001JC001040](https://doi.org/10.1029/2001JC001040), 2003.
- Flaouanas, E., Raveh-Rubin, S., Wernli, H., Drobinski, P., and Bastin, S.: The dynamical structure of intense Mediterranean cyclones, *Clim. Dyn.*, 44, 2411–2427, <https://doi.org/10.1007/s00382-014-2330-2>, 2015.
- Flaouanas, E., Di Luca, A., Drobinski, P., Mailler, S., Arsouze, T., Bastin, S., Beranger, K., and Lebeauin Brossier, C.: Cyclone contribution to the Mediterranean Sea water budget, *Clim. Dyn.*, 46, 913–927, <https://doi.org/10.1007/s00382-015-2622-1>, 2016.
- Flaouanas, E., Fita, L., Lagouvardos, K., and Kotroni, V.: Heavy rainfall in Mediterranean cyclones, Part II. Water budget, precipitation efficiency and remote water sources, *Clim. Dyn.*, 53, 2539–2555, <https://doi.org/10.1007/s00382-019-04639-x>, 2019.
- Flaouanas, E., Davolio, S., Raveh-Rubin, S., Pantillon, F., Miglietta, M. M., Gaertner, M. A., Hatzaki, M., Homar, V., Khodayar, S., Korres, G., Kotroni, V., Kushta, J., Reale, M., and Ricard, D.: Mediterranean cyclones: current knowledge and open questions on dynamics, prediction, climatology and impacts, *Weather Clim. Dynam.*, 3, 173–208, <https://doi.org/10.5194/wcd-3-173-2022>, 2022.
- Flaouanas, E., Aragão, L., Bernini, L., Dafis, S., Doiteau, B., Flocas, H., Gray, S. L., Karwat, A., Kouroutzoglou, J., Lionello, P., Miglietta, M. M., Pantillon, F., Pasquero, C., Patlakas, P., Picornell, M. Á., Porcù, F., Priestley, M. D. K., Reale, M., Roberts, M. J., Saaroni, H., Sandler, D., Scoccimarro, E., Sprenger, M., and Ziv, B.: A composite approach to produce reference datasets for extratropical cyclone tracks: application to Mediterranean cyclones, *Weather Clim. Dynam.*, 4, 639–661, <https://doi.org/10.5194/wcd-4-639-2023>, 2023.
- Gaertner, M. A., Jacob, D., Gil, V., Domínguez, M., Padorno, E., Sánchez, E., and Castro, M.: Tropical cyclones over the Mediterranean Sea in climate change simulations, *Geophys. Res. Lett.*, 34, L14711, <https://doi.org/10.1029/2007GL029977>, 2007.
- Givon, Y.: Mediterranean cyclones: induced evaporation year 2019, TIB AV-Portal [video], <https://doi.org/10.5446/72785>, 2026.
- Givon, Y., Keller Jr., D., Silverman, V., Pennel, R., Drobinski, P., and Raveh-Rubin, S.: Large-scale drivers of the mistral wind: link to Rossby wave life cycles and seasonal variability, *Weather Clim. Dynam.*, 2, 609–630, <https://doi.org/10.5194/wcd-2-609-2021>, 2021.
- Givon, Y., Hess, O., Flaouanas, E., Catto, J. L., Sprenger, M., and Raveh-Rubin, S.: Process-based classification of Mediterranean cyclones using potential vorticity, *Weather Clim. Dynam.*, 5, 133–162, <https://doi.org/10.5194/wcd-5-133-2024>, 2024a.
- Givon, Y., Keller, D., Pennel, R., Drobinski, P., and Raveh-Rubin, S.: Decomposing the role of dry intrusions for ocean evaporation during mistral, *Q. J. R. Meteorol. Soc.*, 150, 1791–1808, <https://doi.org/10.1002/qj.4670>, 2024b.
- Hatzaki, M., Flaouanas, E., Davolio, S., Pantillon, F., Patlakas, P., Raveh-Rubin, S., Hochman, A., Kushta, J., Khodayar, S., Dafis, S., and Liberato M. L. R.: MedCyclones: Working Together toward Understanding Mediterranean Cyclones, *Bull. Amer. Meteor. Soc.*, 104, E480–E487, <https://doi.org/10.1175/BAMS-D-22-0280.1>, 2023.

- Hersbach, H., Bell, B., Berrisford, P., Hirahara, S., Horányi, A., Muñoz-Sabater, J., Nicolas, J., Peubey, C., Radu, R., Schepers, D., Simmons, A., Soci, C., Abdalla, S., Abellan, X., Balsamo, G., Bechtold, P., Biavati, G., Bidlot, J., Bonavita, M., De Chiara, G., Dahlgren, P., Dee, D., Diamantakis, M., Dragani, R., Flemming, J., Forbes, R., Fuentes, M., Geer, A., Haimberger, L., Healy, S., Hogan, R., J., Hólm, E., Janisková, M., Keeley, S., Laloyaux, P., Lopez, P., Lupu, C., Radnoti, G., Rosnay, P., Rozum, I., Vamborg, F., Villaume, S., and Thépaut, L. N.: The ERA5 global reanalysis, *Q. J. R. Meteorol. Soc.*, 146, 1999–2049, <https://doi.org/10.1002/qj.3803>, 2020.
- Hersbach, H., Bell, B., Berrisford, P., Biavati, G., Horányi, A., Muñoz Sabater, J., Nicolas, J., Peubey, C., Radu, R., Rozum, I., Schepers, D., Simmons, A., Soci, C., Dee, D., and Thépaut, J.-N.: ERA5 hourly data on single levels from 1940 to present, Copernicus Climate Change Service (C3S) Climate Data Store (CDS) [data set], <https://doi.org/10.24381/cds.adbb2d47>, 2023.
- Hochman, A., Alpert, P., Kunin, P., Rostkier-Edelstein, D., Harpaz, T., Saaroni, H., and Messori, G.: The dynamics of cyclones in the twentyfirst century: the Eastern Mediterranean as an example, *Clim. Dyn.*, 54, 561–574, <https://doi.org/10.1007/s00382-019-05017-3>, 2020.
- Ilotoviz, E., Ghate, V. P., and Raveh-Rubin, S.: The impact of slantwise descending dry intrusions on the marine boundary layer and air-sea interface over the ARM Eastern North Atlantic site, *J. Geophys. Res.-Atmos.*, 126, e2020JD033879, <https://doi.org/10.1029/2020JD033879>, 2021.
- Jangir, B., Mishra, A., K., and Strobach, E.: The interplay between medicanes and the Mediterranean Sea in the presence of sea surface temperature anomalies, *Atmos. Res.*, 310, 107625, <https://doi.org/10.1016/j.atmosres.2024.107625>, 2024.
- Keller Jr., D.: Fractal Attractor of the Deep Convection Cycle in the Northwest Mediterranean Sea, ESS Open Archive, 10.22541/essoar.174619871.10521682/v1, 2025.
- Keller Jr., D., Givon, Y., Pennel, R., Raveh-Rubin, S., and Drobinski, P.: Untangling the mistral and seasonal atmospheric forcing driving deep convection in the Gulf of Lion: 2012–2013, *Ocean Sci.*, 18, 483–510, <https://doi.org/10.5194/os-18-483-2022>, 2022.
- Keller Jr., D., Givon, Y., Pennel, R., Raveh-Rubin, S., and Drobinski, P.: Untangling the mistral and seasonal atmospheric forcing driving deep convection in the Gulf of Lion: 1993–2013, *J. Geophys. Res.-Oceans*, 129, e2022JC019245, <https://doi.org/10.1029/2022JC019245>, 2024.
- Khodayar, S., Kushta, J., Catto, J. L., Dafis, S., Davolio, S., Ferrarin, C., Flaounas, E., Groenemeijer P., Hatzaki, M., Hochman, A., Kotroni, V., Landa, J., Láng-Ritter, I., Lazoglou, G., Liberato, M. L. R., Miglietta, M. M., Papagiannaki, K., Patlakas, P., Stojanov, R., and Zittis, G.: Mediterranean cyclones in a changing climate: A review on their socio-economic impacts, *Rev. Geophys.*, 63, e2024RG000853, <https://doi.org/10.1029/2024RG000853>, 2025.
- Klaider, N. and Raveh-Rubin, S.: Extended influence of midlatitude cyclones on global cold extremes, *Geophys. Res. Lett.*, 50, e2023GL104999, <https://doi.org/10.1029/2023GL104999>, 2023.
- Lebeauin Brossier, C., Bastin, S., Béranger, K., and Drobinski, P.: Regional mesoscale air–sea coupling impacts and extreme meteorological events role on the Mediterranean Sea water budget, *Clim. Dyn.*, 44, 1029–1051, <https://doi.org/10.1007/s00382-014-2252-z>, 2015.
- Lionello, P. and Giorgi, F.: Winter precipitation and cyclones in the Mediterranean region: future climate scenarios in a regional simulation, *Adv. Geosci.*, 12, 153–158, <https://doi.org/10.5194/adgeo-12-153-2007>, 2007.
- Lionello, P., Boldrin, U., and Giorgi, F.: Future changes in cyclone climatology over Europe as inferred from a regional climate simulation, *Clim. Dyn.*, 30, 657–671, <https://doi.org/10.1007/s00382-007-0315-0>, 2008.
- Miglietta, M. M., Flaounas, E., González-Alemán, J. J., Panegrossi, G., Gaertner, M. A., Pantillon, F., Pasquero, C., Schultz, D., M., D’Adderio, L., P., Dafis, S., Husson, R., Ricchi, A., Carrió, D. S., Davolio, S., Fita, L., Picornell, M., A., Pytharoulis I., Raveh-Rubin, S., Scoccimarro, E., Bernini, L., Cavicchia, L., Conte, D., Ferretti, R., Flocas, H., Gutiérrez-Fernández, J., Hatzaki, M., Santaner, V., H., Jansà, A., and Patlakas, P.: Defining medicanes: Bridging the knowledge gap between tropical and extratropical cyclones in the Mediterranean, *B. Am. Meteorol. Soc.*, 106, E1955–E1971, <https://doi.org/10.1175/BAMS-D-24-0289.1>, 2025.
- Nissen, K. M., Leckebusch, G. C., Pinto, J. G., and Ulbrich, U.: Mediterranean cyclones and windstorms in a changing climate, *Reg. Environ. Change*, 14, 1873–1890, <https://doi.org/10.1007/s10113-012-0400-8>, 2014.
- Papritz, L., Pfahl, S., Sodemann, H., and Wernli, H.: A Climatology of Cold Air Outbreaks and Their Impact on Air–Sea Heat Fluxes in the High-Latitude South Pacific, *J. Climate*, 28, 342–364, <https://doi.org/10.1175/JCLI-D-14-00482.1>, 2015.
- Portal, A., Raveh-Rubin, S., Catto, J. L., Givon, Y., and Martius, O.: Linking compound weather extremes to Mediterranean cyclones, fronts, and airstreams, *Weather Clim. Dynam.*, 5, 1043–1060, <https://doi.org/10.5194/wcd-5-1043-2024>, 2024.
- Portal, A., Angelidou, A., Rousseau-Rizzi, R., Raveh-Rubin, S., Givon, Y., Catto, J. L., Battaglioli, F., Taszarek, M., Flaounas, E., and Martius, O.: Convective Environments Within Mediterranean Cyclones, *Atmos. Sci. Lett.*, 26, e1302, <https://doi.org/10.1002/asl.1302>, 2025.
- Rai, D. and Raveh-Rubin, S.: Enhancement of Indian summer monsoon rainfall by cross-equatorial dry intrusions, *npj Clim. Atmos. Sci.*, 6, 43, <https://doi.org/10.1038/s41612-023-00374-7>, 2023.
- Raveh-Rubin, S.: Dry Intrusions: Lagrangian Climatology and Dynamical Impact on the Planetary Boundary Layer, *J. Climate*, 30, 6661–6682, <https://doi.org/10.1175/JCLI-D-16-0782.1>, 2017.
- Raveh-Rubin, S. and Wernli, H.: Large-scale wind and precipitation extremes in the Mediterranean: a climatological analysis for 1979–2012, *Q. J. Roy. Meteor. Soc.*, 141, 2404–2417, <https://doi.org/10.1002/qj.2891>, 2015.
- Reale, M., Cabos Narvaez, W. D., Cavicchia, L., Conte, D., Coppola, E., Flaounas, E., Giorgi, F., Gualdi, S., Hochman, A., Li, L., Lionello, P., Podrascanin, Z., Salon, S., Sanchez-Gomez, E., Scoccimarro, E., Sein, D. V., and Somot, S.: Future projections of Mediterranean cyclone characteristics using the MedCORDEX ensemble of coupled regional climate system models, *Clim. Dyn.*, 58, 2501–2524, <https://doi.org/10.1007/s00382-021-06018-x>, 2022.
- Reale, O., Feudale, L., and Turato, B.: Evaporative moisture sources during a sequence of floods in the Mediter-

- anean region, *Geophys. Res. Lett.*, 28, 2085–2088, <https://doi.org/10.1029/2000GL012379>, 2001.
- Rieder, J. C., Aemisegger, F., Dente, E., and Armon, M.: Meteorological ingredients of heavy precipitation and subsequent lake-filling episodes in the northwestern Sahara, *Hydrol. Earth Syst. Sci.*, 29, 1395–1427, <https://doi.org/10.5194/hess-29-1395-2025>, 2025.
- Rousseau-Rizzi, R., Raveh-Rubin, S., Catto, J. L., Portal, A., Givon, Y., and Martius, O.: A storm-relative climatology of compound hazards in Mediterranean cyclones, *Weather Clim. Dynam.*, 5, 1079–1101, <https://doi.org/10.5194/wcd-5-1079-2024>, 2024.
- Ruiz, S., Gomis, D., Sotillo, M. G., and Josey, S. A.: Characterization of surface heat fluxes in the Mediterranean Sea from a 44-year high-resolution atmospheric data set, *Global Planet. Change*, 63, 258–274, <https://doi.org/10.1016/j.gloplacha.2007.12.002>, 2008.
- Saaroni, H., Halfon, N., Ziv, B., Alpert, P., and Kutiel, H.: Links between the rainfall regime in Israel and location and intensity of Cyprus lows, *Int. J. Climatol.*, 30, 1014–1025, <https://doi.org/10.1002/joc.1912>, 2010.
- Scoccimarro, E., Borrelli, A., Sangelantoni, L., Cavicchia, L., Tibaldi, S., and Boccaletti, G.: A cul-de-sac effect makes Emilia-Romagna more prone to floods in a changing climate, *Sci. Rep.*, 15, 36823, <https://doi.org/10.1038/s41598-025-24486-7>, 2025.
- Stathopoulos, C., Patlakas, P., Tsalis, C., and Kallos, G.: The Role of Sea Surface Temperature Forcing in the Life-Cycle of Mediterranean Cyclones, *Remote Sens.*, 12, 825, <https://doi.org/10.3390/rs12050825>, 2020.
- Storto, A. and Masina, S.: C-GLORSv5: an improved multipurpose global ocean eddy-permitting physical reanalysis, *Earth Syst. Sci. Data*, 8, 679–696, <https://doi.org/10.5194/essd-8-679-2016>, 2016.
- Strobach, E., Mishra, A. K., Jangir, B., Ziv, B., Sun, R., Siegelman, L., Meroni, A. N., and Klein, P.: Intensification of a rain system imparted by Mediterranean mesoscale eddies, *Sci. Rep.*, 14, 26810, <https://doi.org/10.1038/s41598-024-76767-2>, 2024.
- Thurnherr, I., Hartmuth, K., Jansing, L., Gehring, J., Boettcher, M., Gorodetskaya, I., Werner, M., Wernli, H., and Aemisegger, F.: The role of air–sea fluxes for the water vapour isotope signals in the cold and warm sectors of extratropical cyclones over the Southern Ocean, *Weather Clim. Dynam.*, 2, 331–357, <https://doi.org/10.5194/wcd-2-331-2021>, 2021.
- Tootoonchi, R., Bordoni, S., and D’Agostino, R.: Revisiting the moisture budget of the Mediterranean region in the ERA5 reanalysis, *Weather Clim. Dynam.*, 6, 245–263, <https://doi.org/10.5194/wcd-6-245-2025>, 2025.
- Yu, L.: Global Variations in Oceanic Evaporation (1958–2005): The Role of the Changing Wind Speed, *J. Climate*, 20, 5376–5390, <https://doi.org/10.1175/2007JCLI1714.1>, 2007.
- Zappa, G., Hawcroft, M. K., Shaffrey, L., Black, E., and Brayshaw, D. J.: Extratropical cyclones and the projected decline of winter Mediterranean precipitation in the CMIP5 models, *Clim. Dyn.*, 45, 1727–1738, <https://doi.org/10.1007/s00382-014-2426-8>, 2015.
- Zittis, G., Hadjinicolaou, P., Klangidou, M., Proestos, Y., and Lelieveld, J.: A multi-model, multi-scenario, and multi-domain analysis of regional climate projections for the Mediterranean, *Reg. Environ. Change* 19, 2621–2635, <https://doi.org/10.1007/s10113-019-01565-w>, 2019.
- Zittis, G., Almazroui, M., Alpert, P., Ciais, P., Cramer, W., Dahdal, Y., Fnais, M., Francis, D., Hadjinicolaou, P., Howari, F., Jrrar, A., Kaskaoutis, D. G., Kulmala, M., Lazoglou, G., Mihalopoulos, N., Lin, X., Rudich, Y., Sciare, J., Stenchikov, G., Xoplaki, E., and Lelieveld, J.: Climate change and weather extremes in the Eastern Mediterranean and Middle East, *Rev. Geophys.*, 60, e2021RG000762, <https://doi.org/10.1029/2021RG000762>, 2022.